Attention-Based Multimodal Deep Learning Model for Post-Stroke Motor Impairment Prediction

Rukiye Karakis [1,*], Kali Gurkahraman [2], Georgios D. Mitsis [3], Marie-Hèléne Boudrias [4,5]

[1] Department of Software Engineering, Faculty of Engineering, Sivas Cumhuriyet University, Turkey, rkarakis@cumhuriyet.edu.tr

[2] Department of Computer Engineering, Faculty of Engineering, Sivas Cumhuriyet University, Turkey, kgurkahraman@cumhuriyet.edu.tr

[3] Department of Bioengineering, Faculty of Engineering, McGill University, Montreal, QC, Canada, georgios.mitsis@mcgill.ca

[4] School of Physical and Occupational Therapy, Faculty of Medicine and Health Sciences, McGill University, Montreal, QC, Canada, mh.boudrias@mcgill.ca

[5] BRAIN Laboratory, Jewish Rehabilitation Hospital, Site of Centre for Interdisciplinary Research of Greater Montreal (CRIR) and CISSS-Laval, QC, Canada

Abstract. Accurately predicting post-stroke motor impairment remains a challenge due to the complexity of functional recovery and its association with neuroimaging biomarkers. This study presents a deep learning (DL) framework that integrates Magnetic Resonance Imaging (MRI)-based measures such as Diffusion Tensor Imaging (DTI) metrics—fractional anisotropy (FA), mean diffusivity (MD), radial diffusivity (RD), and axial diffusivity (AD)—along with white matter (WM) and gray matter (GM) intensities to classify upper limb motor function. Unlike previous approaches, the proposed model directly extracts whole-brain volumetric features without predefined region-of-interest constraints. Feature representation is enhanced using residual connections, attention mechanisms, and Global Average Pooling (GAP), improving classification performance while maintaining computational efficiency. The ensemble framework combines six independently trained models to optimize multi-modality integration. The results demonstrate that the WM+FA combination achieved the highest accuracy (0.97), outperforming the full ensemble model (0.96). These findings exceed the performance reported in prior studies, emphasizing the effectiveness of microstructural and structural biomarkers in motor recovery prediction. This optimized DL framework has the potential to improve post-stroke motor impairment classification, supporting early rehabilitation planning, and personalized treatment strategies.

Keywords: Deep Learning, Diffusion Tensor Imaging, Feature Fusion, Magnetic Resonance Imaging, Multimodal Learning, Upper-limb Motor Impairment.

1 Introduction

Stroke is a leading cause of death and disability worldwide, causing motor, cognitive, and speech impairments due to disrupted cerebral blood flow [1]. Despite advances in acute care, effective rehabilitation remains crucial [1-2]. Tools like the National Institutes of Health Stroke Scale (NIHSS) and Fugl-Meyer Assessment (FMA) assess clinical function but overlook neurobiological mechanisms, leading to variable outcomes based on brain damage and individual differences [3-9].

Neuroimaging biomarkers, particularly diffusion tensor imaging (DTI) metrics and structural features of white matter (WM) and gray matter (GM), are crucial for predicting motor recovery after stroke [3, 5-11]. DTI assesses WM integrity, with metrics like fractional anisotropy (FA), mean diffusivity (MD), radial diffusivity (RD), and axial diffusivity (AD) reflecting microstructural damage and recovery [5,7-8]. Additionally, GM structures such as the primary motor cortex, supplementary motor area, and premotor cortex are linked to functional recovery [9]. Combining WM and GM markers enables a comprehensive assessment of recovery potential.

Traditional models like PREP [12] and PREP2 [13] combine clinical scores with transcranial magnetic stimulation and Magnetic Resonance Imaging (MRI) features. While clinically interpretable, they rely on predefined biomarkers and expert-driven feature selection, limiting their ability to capture brain reorganization. Their moderate accuracy (0.70-0.80) suggests that clinical measures alone may not ensure robust prediction. As summarized in Table 1, recent studies explored multimodal neuroimaging with machine learning (ML) using T1-weighted (T1w) MRI, functional MRI (fMRI), diffusion-weighted imaging (DWI), and corticospinal tract (CST) integrity [14]. While promising, most rely on traditional statistical methods, limiting their ability to model complex biomarker interactions. Tozlu et al. [15] reported high regression (R^2: 0.70–0.91) but low classification performance (area under the curve, AUC: 0.50–0.63), while Rehme et al. [16] showed resting-state fMRI improved classification accuracy (Acc: 0.83–0.88) compared to lesion-based diffusion MRI with lower performance (0.74). Rondina et al. [17] used Gaussian Process Regression (GPR) and Support Vector Machine (SVM), achieving correlations of 0.68–0.83, highlighting the importance of feature selection. However, most ML models rely on predefined biomarkers and expert-driven feature selection, limiting adaptability and generalizability. Deep learning (DL) models, such as multi-channel 3D-Convolutional Neural Networks (CNNs) integrating DTI maps, WM and GM integrity, and demographic data, achieved the highest performance (Acc: 0.92, AUC: 0.92) [18], though challenges in balancing multi-modal feature contributions and preventing modality dominance remain major challenges.

Accurately predicting post-stroke motor impairment remains challenging due to the complex interactions between neuroimaging biomarkers and functional recovery. This study proposes a DL framework that integrates DTI metrics (FA, MD, RD, AD), structural MRI-derived WM and GM intensity values, and demographic data (age, gender, stroke time) to classify upper limb motor function as Good or Poor based on the FMA [3, 19]. Unlike conventional methods, our model utilizes a whole-brain analysis approach, where volumetric features are extracted directly from neuroimaging data without predefined region-of-interest (ROI) constraints. Feature extraction is refined using

Global Average Pooling (GAP), the Convolutional Block Attention Module (CBAM), and residual connections to enhance motor-relevant representations. Six independent models were trained to improve robustness, each specializing in a different imaging modality, and combined their outputs using a weighted ensemble learning strategy, improving classification accuracy and generalizability. The main contributions of this study are as follows:

- Integrating DTI-derived diffusion metrics, structural MRI features, and demographic data to comprehensively represent post-stroke motor impairment.
- Implementing a whole-brain analysis approach, avoiding predefined ROI constraints for improved feature representation.
- Optimizing feature fusion using GAP, CBAM-based attention, and residual connections to enhance feature extraction.
- Combining outputs from six independent models using a weighted ensemble learning approach to enhance robustness.
- Achieving promising classification accuracy using a multimodal DL approach, with potential to support early rehabilitation planning and personalized treatment strategies.

Table 1. Comparison of ML and DL approaches for post-stroke motor impairment prediction.

Study	Method	Input Data	Output	Performance
Rondina et al. [17]	GPR, SVM	T1w-MRI, fMRI, lesion location, CST integrity	Motor function scores	R: 0.68–0.83
Tozlu et al. [15]	Elastic-Net, RF, ANN, SVM, Decision Trees	Demographics, clinical data, TMS-based neurophysiology, regional dysconnectivity (T1-MRI)	FMA scores, upper limb motor impairment class	R^2: 0.70–0.91, AUC: 0.50–0.63
Rehme et al. [16]	SVM	Resting-state fMRI, DWI lesion maps, connectivity maps	Hand motor impairment classification	Acc*: 0.83–0.88 (fMRI), 0.74 (DWI)
Karakis et al. [18]	Multi-Channel 3D-CNN, SVM	FA, MD, RD, AD, GM and WM integrity (MRI), demographic data	Upper limb motor impairment class	Acc: 0.92 (CNN), 0.91 (SVM) AUC: 0.92

*Acc: Accuracy

2 Materials and Methods

Fig. 1 illustrates the proposed multimodal DL framework for post-stroke motor impairment classification. The model integrates DTI, MRI, and demographic data, extracting FA, MD, RD, and AD maps from DTI and WM/GM segmentations from MRI. Features are refined using CBAM layers and residual connections, then processed through GAP, FCLs, and softmax for classification. Predictions from all pathways are combined using a weighted ensemble model to enhance classification robustness.

2.1 Dataset

Multiple independent datasets [18] were used to evaluate the proposed DL framework, incorporating DTI, structural MRI, and patient-specific clinical attributes. The dataset

consisted of 154 neuroimaging scans from 123 individuals, including both stroke patients and healthy participants. Motor impairment severity was classified into Good (n=101) and Poor (n=53) groups based on validated clinical assessments. A total of 64 scans were acquired in the chronic phase, while 31 were obtained in the subacute phase.

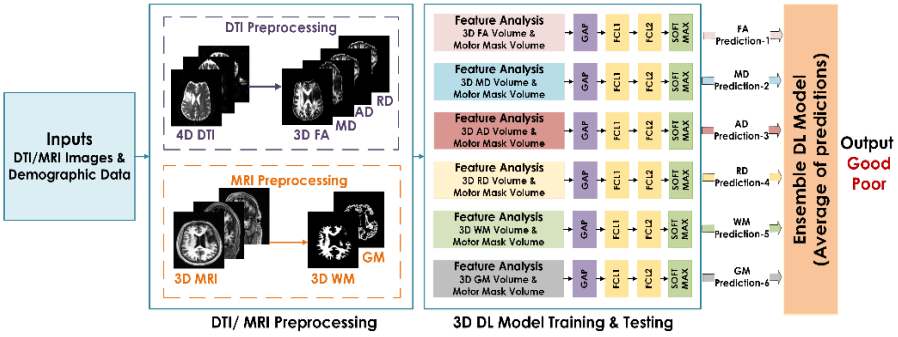

Fig. 1. Multimodal deep learning framework for post-stroke motor impairment classification.

DTI scans were acquired using 3T MRI systems with single-shot EPI sequences, employing b-values between 700 and 1000 s/ mm^2 across different protocols. Each scan included 30–61 non-collinear diffusion directions and at least one low b-value volume (b=0 or b=100 s/mm^2) for baseline diffusion estimation. Voxel resolutions varied across datasets: 1.72×1.72×1.72 mm^3, 2.0×2.0×2.0 mm^3, and 1.8×1.8×2.0 mm^3, ensuring high spatial fidelity for fiber tracking and microstructural assessment. Structural MRI scans were acquired with voxel sizes of 1×1×1 mm^3, 1×1×1 mm^3, and 0.45×0.45×0.90 mm^3, enabling segmentation, lesion characterization, and volumetric analysis [2, 10, 11].

Motor impairment was evaluated using validated clinical scales, including FMA [19], Box and Block Test (BBT) [20], Nine-Hole Peg Test (NHPT) [21], and Grip Strength (GS) [22]. When multiple motor scores were available, principal component analysis (PCA) was applied to derive a single representative measure, a strategy previously used in post-stroke recovery studies [23-24]. Participants were classified into good and poor recovery groups based on statistical thresholds derived from mean and median analyses of FMA and PCA scores, aligning with established cutoff values in the literature [24].

2.2 Data Preprocessing

DTI images were denoised using the *dwidenoise()* function in MRtrix. Motion and eddy current distortions were corrected using *eddy_correct()* in FSL, with b-vector rotations applied to preserve orientation integrity [25]. The BET tool in FSL was used for skull stripping, and diffusion metrics (FA, MD, RD, AD) were computed with dtifit in FSL. All maps were registered to a standard DTI template using *FLIRT* + *FNIRT* (FSL). To ensure lesion alignment, images of patients with left-hemisphere lesions were flipped using *fslswapdim()* in FSL [2]. T1/T2-weighted MRI images were reoriented using *fslreorient2std()*, denoised using BM4D filtering [26] in MATLAB, and skull-stripped

with BET (FSL). Bias field correction was performed using FAST (FSL), and images were non-linearly registered to the MNI 2 mm template (FLIRT + FNIRT in FSL). For lesion alignment, left-hemisphere lesion scans were flipped. WM, GM, and cerebrospinal fluid (CSF) segmentation was carried out using FAST (FSL).

2.3 Multimodal Deep Learning Model

The proposed DL model consists of four primary blocks, each designed to enhance feature extraction through convolutional operations, residual learning, and attention mechanisms (Fig. 2). Block 1 applies a standard 3D convolution with batch normalization (BN) and ReLU activation, avoiding pooling to preserve spatial resolution. Block 2 introduces residual connections to facilitate gradient flow and feature reuse while avoiding pooling to retain fine-grained spatial details. Block 3 integrates residual learning and CBAM to enhance feature representation by selectively focusing on the most relevant spatial and channel-wise information [27]. Additionally, 3D average pooling is applied to reduce redundant information and improve generalization. Block 4 incorporates CBAM and GAP but omits residual connections, ensuring effective feature aggregation before classification.

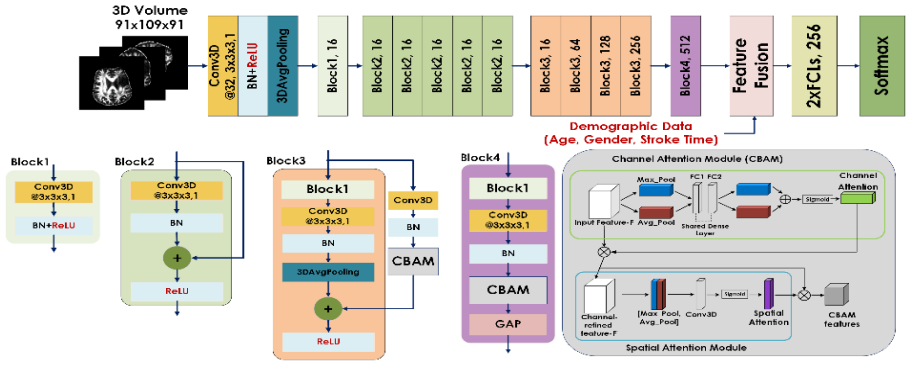

Fig. 2. Proposed deep learning model with residual connections and CBAM-enhanced feature extraction.

The CBAM enhances feature extraction by applying channel attention and spatial attention mechanisms sequentially [27]. Given an input feature map F, channel attention learns the importance of each channel by applying GAP and Global Max Pooling (GMP). These pooled features pass through a shared multilayer perceptron (MLP) and sigmoid activation, generating a channel attention map $M_C(F)$, formulated as:

$$M_C(F) = \sigma\left(MLP\big(GAP(F)\big) + MLP\big(GMP(F)\big)\right) \quad (1)$$

where σ denotes the sigmoid function, and MLP consists of two FCLs. The input feature map is then refined by element-wise multiplication with $M_C(F)$. Next, spatial attention focuses on key spatial regions by pooling along the channel dimension, followed by a 7x7x7 and a sigmoid activation, producing the spatial attention map $M_s(F')$:

$$M_s(F') = \sigma\left(f^{7\times7\times7}([GAP(F'); GMP(F')])\right) \quad (2)$$

where $f^{7\times7\times7}$ represents the convolution operation. The final enhanced feature map F'' is obtained by multiplying $M_s(F')$ with the refined feature map:

$$F'' = M_s(F') \otimes M_c(F) \otimes F \quad (3)$$

By integrating CBAM in Blocks 3 and 4, the model effectively emphasizes critical features, improving feature representation and classification performance for post-stroke motor impairment prediction. CBAM is particularly advantageous in multimodal brain image analysis, as it enhances the model's ability to capture relevant spatial and channel-wise dependencies across different neuroimaging modalities [28-29].

2.4 Performance Metrics and Implementation

The proposed model was evaluated using accuracy, specificity, precision, recall, and F1-score. It was implemented in Python using Keras with TensorFlow and trained with Adam (momentum: 0.9, learning rate: 0.0001, weight decay: 0.00001). Dropout and L2 regularization were applied to prevent overfitting. The experiments ran on an NVIDIA RTX A6000 (48 GB GPU) with 64 GB RAM. An 80-20 train-test split was used, with 154 samples (101 Good, 53 Poor) divided using 10-fold repeated random subsampling validation (RSV). RSV ensured balanced test data and multiple training appearances for each sample. To address class imbalance, sharpening-based data augmentation was applied. The model was trained 10 times with different RSV splits, totaling 100 iterations for validation.

This study's code implementations, trained model weights, and sample test images are available at *https://github.com/miccai3806/MotorImpairmentPrediction*.

3 Results and Discussion

Table 2 presents the performance values of different imaging modalities for motor impairment classification. WM achieved the highest accuracy (0.910), followed by FA (0.887) and AD (0.877), while GM had the lowest (0.827). FA and AD also demonstrated strong specificity and precision, contributing to their overall classification performance. GM and WM maps provided tissue-specific features important for stroke recovery. Our trials yielded lower performance for whole-intensity maps. This separation may enable the model to focus on detailed cortical (GM) and connectivity (WM) patterns without explicit ROI selection.

Table 3 presents the performance of different ensemble approaches for motor impairment classification. The WM+FA combination achieved the highest accuracy (0.973) and F1-score (0.972), outperforming the full ensemble model (0.957). This aligns with the literature, where FA and WM are key biomarkers for motor recovery prediction, capturing both microstructural and structural brain changes [3, 5-9]. Specificity remained consistently high (≥0.98) across all configurations while excluding GM and MD led to the lowest performance, highlighting their contribution to classification. Overall, ensemble learning improved robustness, with certain modality combinations

yielding superior results. In contrast to early fusion approaches such as Karakis et al. [18], who used a multi-channel CNN and reported 0.92 accuracy, our ensemble method addresses the feature fusion challenge by integrating modality-specific predictions at the decision level. This strategy ensures more balanced contributions from each modality, as no single modality dominates the final outcome. Importantly, it reduces the overlap of misclassified cases, since what one modality fails to detect is often captured by another. This highlights the complementary nature of the modalities and demonstrates the advantage of decision-level fusion in improving overall classification performance. While diffusion metrics appear correlated, in our ensemble what matters is which cases are misclassified by each modality. FA and MD, though related, capture distinct properties; in our cohort, lesions often spare motor pathways, so FA reductions outside these areas may not reflect motor impairment, while MD increases in non-motor regions may mislead. WM+FA yielded the best performance, supporting their clinical relevance. WM and GM maps provide tissue-specific features important for stroke recovery. Our trials showed they outperform whole-intensity maps.

Table 2. Performance values for imaging modalities in motor impairment classification.

Modality	Accuracy	Recall	Specificity	Precision	F1
WM	**0.910***	**0.907**	**0.913**	**0.918**	**0.910**
	[0.833 0.967]	**[0.867 0.933]**	**[0.800 1.0]**	**[0.813 1.0]**	**[0.839 0.966]**
GM	0.827	0.867	0.787	0.808	0.834
	[0.767 0.933]	[0.733 0.933]	[0.800 0.933]	[0.786 0.933]	[0.759 0.933]
FA	**0.887**	**0.867**	**0.907**	**0.905**	**0.883**
	[0.833 0.967]	**[0.800 1.0]**	**[0.867 0.933]**	**[0.857 0.938]**	**[0.828 0.968]**
AD	0.877	0.866	0.873	0.871	0.863
	[0.800 0.933]	[0.867 0.933]	[0.667 1.0]	[0.737 1.0]	[0.824 0.929]
MD	0.853	0.860	0.847	0.857	0.855
	[0.733 0.933]	[0.733 0.933]	[0.733 0.933]	[0.733 0.933]	[0.733 0.933]
RD	0.863	0.880	0.847	0.863	0.865
	[0.767 0.933]	[0.933 0.933]	[0.600 0.933]	[0.700 0.933]	[0.800 0.933]

*Average [min max]

Table 3. Performance values of ensemble approaches with different model combinations for motor impairment classification.

Model Combination	Accuracy	Recall	Specificity	Precision	F1
All Models (EM6)	0.957*	0.913	1.0	1.0	0.953
	[0.900 1.0]	[0.800 1.0]	[1.0 1.0]	[1.0 1.0]	[0.889 1.0]
WM+FA+AD+RD+MD	0.957	0.913	1.0	1.0	0.953
(EM5)	[0.900 1.0]	[0.800 1.0]	[1.0 1.0]	[1.0 1.0]	[0.889 1.0]
WM+FA+AD+RD (EM4)	0.927	0.873	0.980	0.978	0.922
	[0.900 1.0]	[0.800 1.0]	[1.0 1.0]	[1.0 1.0]	[0.889 1.0]
WM+FA+AD (EM3)	0.940	0.900	0.980	0.979	0.936
	[0.900 1.0]	[0.867 1.0]	[0.933 1.0]	[0.929 1.0]	[0.897 1.0]
WM+FA (EM2)	**0.973**	**0.947**	**1.0**	**1.0**	**0.972**
	[0.933 1.0]	**[0.867 1.0]**	**[1.0 1.0]**	**[1.0 1.0]**	**[0.929 1.0]**

*Average [min max]

The proposed ensemble DL model outperforms previous methods, achieving 0.97 accuracy with the WM+FA combination and 0.96 accuracy when integrating all modalities (WM, FA, AD, RD, and MD). As shown in Figure 3, certain modality combinations yield higher accuracy than full integration, highlighting the importance of modality selection. This aligns with the findings in Table 1, where DL models incorporating multi-modal neuroimaging data outperform traditional ML approaches. The results reinforce the significance of FA and WM as key biomarkers for motor recovery prediction, capturing both microstructural and structural brain changes.

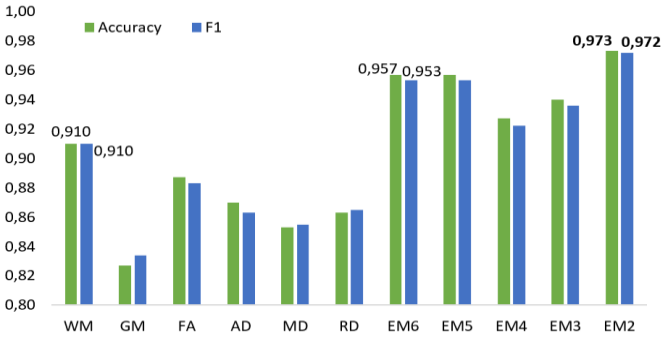

Fig. 3. Accuracy and F1-score values of modalities and ensemble models (EM).

The absence of an external validation cohort limits the generalizability of the model and raises concerns about potential overfitting. To address this risk and enhance feature focus, the model integrates CBAM attention, residual connections, L2 regularization, dropout, and modality-specific training. In addition, multiple independent datasets were used to provide heterogeneity and reduce the likelihood of overfitting. Our finding that WM+FA maps provide strong predictive power is consistent with previous studies linking FA and WM integrity to motor recovery [13]. However, given the absence of external validation in this study, it remains important to confirm these results in independent cohorts to ensure reproducibility.

While PCA-derived composite scores facilitated harmonization of motor assessments across heterogeneous datasets, this approach may reduce granularity in clinical outcome interpretation by obscuring individual test variances. Given challenges in collecting stroke cohorts and using different motor assessments, PCA was applied to harmonize these measures, consistent with prior studies [17, 23].

4 Conclusion

Predicting motor impairment after stroke remains challenging due to the complexity of integrating neuroimaging biomarkers. This study introduced an ensemble DL model leveraging multimodal MRI and DTI-derived features, achieving 0.97 accuracy with WM+FA and 0.96 with the full ensemble. These results underscore the importance of both microstructural and structural imaging in motor recovery prediction. Unlike con-

ventional ML approaches that require manual feature selection, our method automatically learns discriminative patterns from whole-brain data. Future work will aim to enhance feature fusion, incorporate motor regions, and refine ensemble learning for improved clinical applicability. Misclassified cases from single-modality models will be logged and analyzed to confirm low overlap and validate the ensemble's complementary nature. The ensemble's weight distribution and modality-specific contributions will be reported to quantify importance at the decision level. Feature relevance will be explored through attention maps and interpretability tools to better understand model decision. Although the model includes demographic variables, no clinical-only baseline was added; inclusion in future studies may provide further insights.

Acknowledgments. We thank Dr. Lara A. Boyd (University of British Columbia, Canada), Dr. Adrian G. Guggisberg (University of Geneva, Switzerland), and Dr. Nick Ward (UCL Institute of Neurology, United Kingdom) for providing the data. Data from the Boyd lab were collected with support from the Canadian Institutes of Health Research (MOP-130269). This work was funded by the Scientific and Technological Research Council of Turkey (TUBITAK-2219) [RK], the Scientific Research Project Fund of Sivas Cumhuriyet University (Project No. TEKNO-2023-038) [RK], the Canadian Foundation for Innovation (grant no. 34277) [MHB], and the Fonds de recherche du Québec–Santé (FRQ-S) Research Scholar Award [MHB].

Disclosure of Interests. The authors have no competing interests to declare that are relevant to the content of this article.

References

1. Kim, Y.W.: Update on stroke rehabilitation in motor impairment. Brain & Neurorehabilitation **15**(2), e12 (2022)
2. Larivière, S., Ward, N.S., Boudrias, M.H.: Disrupted functional network integrity and flexibility after stroke: Relation to motor impairments. NeuroImage Clinical **19**, 883–891 (2018)
3. Boyd, L. A., Hayward, K. S., Ward, N. S., Stinear, C. M., Rosso, C., Fisher, R. J., Carter, A. R., Leff, A. P., Copland, D. A., Carey, L. M., Cohen, L. G., Basso, D. M., Maguire, J. M., & Cramer, S. C.: Biomarkers of stroke recovery: consensus-based core recommendations from the stroke recovery and rehabilitation roundtable. International Journal of Stroke **12**(5), 480-493 (2017)
4. Milot, M.H., Cramer, S.C.: Biomarkers of recovery after stroke. Current opinion in neurology **21**(6), 654-659 (2008)
5. Moura, L. M., Luccas, R., de Paiva, J. P. Q., Amaro, E., Jr, Leemans, A., Leite, C. D. C., Otaduy, M. C. G., Conforto, A. B.: Diffusion tensor imaging biomarkers to predict motor outcomes in stroke: a narrative review. Frontiers in Neurology **10**, 445 (2019)
6. Tavazzi, E., Bergsland, N., Pirastru, A., Cazzoli, M., Blasi, V., Baglio, F.: MRI markers of functional connectivity and tissue microstructure in stroke-related motor rehabilitation: A systematic review. NeuroImage: Clinical **33**, 102931 (2022)
7. Puig, J., Blasco, G., Schlaug, G., Stinear, C. M., Daunis-I-Estadella, P., Biarnes, C., Figueras, J., Serena, J., Hernández-Pérez, M., Alberich-Bayarri, A., Castellanos, M., Liebeskind, D. S., Demchuk, A. M., Menon, B. K., Thomalla, G., Nael, K., Wintermark, M., Pedraza, S.: Diffusion tensor imaging as a prognostic biomarker for motor recovery and rehabilitation after stroke. Neuroradiology **59**, 343-351 (2017)

8. Werring, D.J., Toosy, A.T., Clark, C.A., Parker, G.J., Barker, G.J., Miller, D.H., Thompson, A.J.: Diffusion tensor imaging can detect and quantify corticospinal tract degeneration after stroke. Journal of Neurology, Neurosurgery & Psychiatry **69**(2), 269-272 (2000)
9. Yang, M., Yang, Y. R., Li, H. J., Lu, X. S., Shi, Y. M., Liu, B., Chen, H. J., Teng, G. J., Chen, R., Herskovits, E. H.: Combining diffusion tensor imaging and gray matter volumetry to investigate motor functioning in chronic stroke. PLoS One **10**(5), e0125038 (2015)
10. Hayward, K.S., Neva, J.L., Mang, C.S., Peters, S., Wadden, K.P., Ferris, J.K., Boyd, L.A.: Interhemispheric Pathways Are Important for Motor Outcome in Individuals with Chronic and Severe Upper Limb Impairment Post Stroke. Neural plasticity **2017**, 4281532 (2017)
11. Guggisberg, A.G., Nicolo, P., Cohen, L.G., Schnider, A., Buch, E.R.: Longitudinal structural and functional differences between proportional and poor motor recovery after stroke. Neurorehabilitation and neural repair **31**(12), 1029–1041 (2017)
12. Stinear, C.M., Barber, P.A., Petoe, M., Anwar, S., Byblow, W.D.: The PREP algorithm predicts potential for upper limb recovery after stroke. Brain **135**, 2527–2535 (2012)
13. Stinear, C.M., Byblow, W.D., Ackerley, S.J., Smith, M.C., Borges, V.M., Barber, P.A.: PREP2: A biomarker-based algorithm for predicting upper limb function after stroke. Annals of clinical and translational neurology **4**(11), 811–820 (2017)
14. Diamandi, J., Raimondo, C., Piper, K., Roy, J., Serva, S., Alizadeh, M., Flanders, A., Tjoumakaris, S., Gooch, R., Jabbour, P., Rosenwasser, R., Mouchtouris, N.: Use of multimodal non-contrast MRI to predict functional outcomes after stroke: A study using DP-pCASL, DTI, NODDI, and MAP MRI. NeuroImage: Clinical, 103742 (2025)
15. Tozlu, C., Edwards, D., Boes, A., Labar, D., Tsagaris, K.Z., Silverstein, J., Pepper Lane, H., Sabuncu, M.R., Liu, C., Kuceyeski, A.: Machine learning methods predict individual upper-limb motor impairment following therapy in chronic stroke. Neurorehabilitation and Neural Repair **34**(5), 428-439 (2020)
16. Rehme, A.K., Volz, L.J., Feis, D.L., Bomilcar-Focke, I., Liebig, T., Eickhoff, S.B., Fink, G. R., Grefkes, C.: Identifying Neuroimaging Markers of Motor Disability in Acute Stroke by Machine Learning Techniques. Cerebral cortex **25**(9), 3046–3056 (2015)
17. Rondina, J.M., Park, C.H., & Ward, N.S.: Brain regions important for recovery after severe post-stroke upper limb paresis. Journal of neurology, neurosurgery, and psychiatry **88**(9), 737–743 (2017)
18. Karakis, R., Gurkahraman, K., Mitsis, G.D., Boudrias, M.H.: Deep learning prediction of motor performance in stroke individuals using neuroimaging data. Journal of Biomedical Informatics **141**, 104357 (2023)
19. Fugl-Meyer, A.R., Jääskö, L., Leyman, I., Olsson, S., Steglind, S.: The post-stroke hemi-237 plegic patient a method for evaluation of physical performance. Scand J. Rehabil. Med. **7**(1), 13-31 (1975)
20. Mathiowetz, V., Volland, G., Kashman, N., Weber, K.: Adult norms for the box and block test of manual dexterity. Am. J. Occup. Ther. **39**, 386–391 (1985)
21. Mathiowetz, V., Weber, K., Kashman, N., Volland, G.: Adult norms for the nine hole peg test of finger dexterity. The Occupational Therapy Journal of Research 5 (1), 24–38 (1985)
22. Mathiowetz, V., Weber, K., Volland, G., Kashman, N.: Reliability and validity of grip and pinch strength evaluations. J. Hand Surg. **9**(2), 222–226 (1984)
23. Rondina, J.M., Filippone, M., Girolami, M., Ward, N.S.: Decoding post-stroke motor function from structural brain imaging. NeuroImage Clinical **12**, 372–380 (2016)
24. Woytowicz, E.J., Rietschel, J.C., Goodman, R.N., Conroy, S.S., Sorkin, J.D., Whitall, J., McCombe Waller, S., Determining levels of upper extremity movement impairment by applying a cluster analysis to the Fugl-Meyer assessment of the upper extremity in chronic stroke. Archives of Physical Medicine and Rehabilitation **98**(3), 456-462 (2017)

25. Soares, J.M., Marques, P., Alves, V., Sousa, N.: A hitchhiker's guide to diffusion tensor imaging. Front Neurosci. **7**, 31 (2013)
26. Mäkinen, Y., Azzari, L., Foi, A.: Collaborative filtering of correlated noise: Exact transform-domain variance for improved shrinkage and patch matching. IEEE Transactions on Image Processing **29**, 8339-8354 (2020)
27. Woo, S., Park, J., Lee, J.Y., Kweon, I.S.: Cbam: Convolutional block attention module. In: Proceedings of the European conference on computer vision (ECCV), pp. 3-19. (2018).
28. Li, T., Guo, Y., Zhao, Z., Chen, M., Lin, Q., Hu, X., Yao, Z., Hu, B.: Automated diagnosis of major depressive disorder with multi-modal MRIs based on contrastive learning: a few-shot study. IEEE Transactions on Neural Systems and Rehabilitation Engineering **32**, 1566-1576 (2024)
29. Liu, J., Chen, S., Chen, J., Wang, B., Zhang, Q., Xiao, L., Zhang, D., Cai, X.: Structural brain connectivity guided optimal contact selection for deep brain stimulation of the subthalamic nucleus. World Neurosurgery **188**, e546-e554 (2024)